Adsorption thermodynamics and kinetic investigation of aromatic amphoteric compounds onto different polymeric adsorbents

WANG Hai-ling[1,2,*], FEI Zheng-hao[2], CHEN Jin-long[3],
ZHANG Quan-xing[3], XU Yan-hua[1]

1. College of Environment, Nanjing University of Technology, Nanjing 210009, China. E-mail: wanghailing@nju.org.cn
2. Jiangsu Provincial Key Laboratory of Coastal Wetland Bioresources and Environmental Protection, Yancheng 224002, China
3. State Key Laboratory of Pollution Control and Resources Reuse, School of Environment, Nanjing University, Nanjing 210093, China

Abstract

The adsorption behavior of p-aminobenzoic acid and o-aminobenzoic acid onto the different polymeric adsorbents was systematically investigated as a function of the solution concentration and temperature. Experimental results indicated that the equilibrium adsorption data of the four polymeric adsorbents fitted well in the Freundlich isotherm. The adsorption capacity of multi-functional polymeric adsorbent NJ-99 was the highest, which might be attributed to the strong hydrogen-bonding interaction between the amino groups on the resin and the carboxyl group of aminobenzoic acid. The adsorption capacity of o-aminobenzoic acid onto any adsorbent was higher than p-aminobenzoic acid. Thermodynamic studies suggested the exothermic, spontaneous physical adsorption process. Adsorption kinetics results showed that the adsorption followed the pseudo-second-order kinetics model and the intraparticle mass transfer process was the rate-controlling step.

Key words: aromatic amphoteric compound; aminobenzoic acid; polymeric adsorbents; adsorption; thermodynamics; kinetics

Introduction

Wastewater containing aromatic compounds presents a serious disposal problem because of its toxicity and poor biodegradation as well as good solubility in water. Especially for the aromatic amphoteric compounds involving both Lewis acid and Lewis base functional groups, their particular physicochemical characteristics bring more difficulties for the treatment of wastewater. A lot of methods, such as biological degradation and oxidation (Zhang *et al.*,1999; Lin *et al.*, 2001), applied for the purification of water contaminated by aromatic amphoteric compounds, are often with limited success. Resin adsorption technology has been used as a more attractive alternative for removing aromatic pollutants from wastewater (He and Huang, 1995; Zhang *et al.*, 2001). Many studies (Pan *et al.*, 2005; Cai *et al.*, 2005) have been conducted on the removal of phenols and aromatic amines involving one kind of functional group. However, the concerned research on the resin adsorption techniques of aromatic amphoteric compounds has not been systematically investigated.

Mass transfer within the resin particles can be complex,

as adsorption is inherently a transient process involving some short-range diffusion in both the fluid and the adsorbed phases. Both intraparticle and external diffusion may play a role in the liquid phase adsorption on porous adsorbents. Although a large number of studies on the adsorption kinetics have been reported (Annadurai and Krishnan, 1997; Ho and Mckay, 1999; Mckay and Ho, 1999; Li and Arup, 2000), few of them addressed the adsorption thermodynamics and kinetics of aromatic amphoteric compounds on polymeric adsorbents.

The current study aimed at identifying the significance of intraparticle and external diffusion of the aromatic amphoteric compound aminobenzoic acid inside the water-compatible hypercrosslinked multi-functional polymeric adsorbent NJ-99 and NG-10 in comparison with the hypercrosslinked adsorbent CHA-111 and the hydrophobic macroporous adsorbent XAD-4. Thermodynamic investigations have been performed to elucidate the equilibrium adsorption behavior of aminobenzoic acid onto polymeric adsorbents.

1 Materials and methods

1.1 Materials

Two kinds of aminobenzoic acid (p-aminobenzoic acid and o-aminobenzoic acid) were purchased from Shanghai

Chemical Reagent Station (Shanghai, China) and used in the study without further purification, which were all dissolved in deionized water. The physical properties are listed in Table 1. Adsorbent Amberlite XAD-4 was purchased from the Beijing Branch of Rohm Haas Company (Beijing, China). Adsorbents CHA-111, NJ-99 and NG-10 were obtained from Jiangsu N&G Environmental Technology Co. Ltd. (Jiangsu, China).

Table 1 Physical properties of the adsorbates

Adsorbate	Water solubility (wt%)[a]	pK_{a_1}	pK_{a_2}
p-Aminobenzoic acid	0.59	2.38	4.89
o-Aminobenzoic acid	0.16	2.11	4.95

[a] Liu *et al.*, 2002.

1.2 Characterization of adsorbents

The special hypercrosslinked polymeric adsorbent CHA-111 was prepared by controlling the post-crosslinking reaction, whereas NJ-99 and NG-10 were obtained by introducing some amino groups and sulfonic groups, respectively, to the surface of porous polystyrene-divinylbenzene beads during the post-crosslinking process.

The specific surface area and the pore structure of the four polymeric adsorbents were measured using a Micromeritcs apparatus (ASAP-2010 Micromeritcs Instrument Corporation, USA) with nitrogen as sorbate following the Brunauer Emmett Teller (BET) method. Infrared spectra of the polymeric adsorbents were obtained from a Nicolet 170 SX IR spectrometer (USA) with a pellet of powdered potassium bromide and resin. The amounts of amino groups on adsorbent NJ-99 and the sulfonic groups on adsorbent NG-10 matrix were measured as reported in the reference (He and Huang, 1995).

1.3 Adsorption static test

Prior to their initial use, the four polymeric adsorbents were first extracted by ethanol in a Soxhlet apparatus for 8 h and then dried under vacuum at 333 K for 8 h. The static adsorption of the aromatic amphoteric compound aminobenzoic acid on the adsorbents at three different temperatures (283, 298 and 313 K) was conducted as follows: 0.100 g of the dry resin was introduced into an airproof flask. 100 ml aqueous solution of aminobenzoic acid with initial concentrations (C_0) of 200, 400, 600, 800, 1000, 1200, and 1400 mg/L were then added into

each flask. The flasks were consequently placed in a Constant Temperature Shaker (ZD-88-4, Taicang Guangming Experimental Instrument Co. Ltd., Jiangsu Province, China) at a pre-settled temperature and equilibrated at 150 r/min for 24 h. Finally, the equilibrium concentrations (C_e) of the adsorbate were determined by a Helious Betra UV-Vis spectrometer (UK) at 275 nm (*p*-aminobenzoic acid) or 224 nm (*o*-aminobenzoic acid). The equilibrium adsorption capacities Q_e (mmol/g) were thus calculated with Eq. (1):

$$Q_e = V_1(C_0 - C_e)/WM \qquad (1)$$

where, V_1 is the volume of solution (L), W is the mass of dry resin (g), and M is the molecular weight of the adsorbate.

1.4 Adsorption kinetic test

Adsorption kinetic test of aminobenzoic acid on the four adsorbents was carried out in a way similar to the static adsorption test, except that 0.100 g of the dry resin was introduced into 100 ml aqueous solution of aminobenzoic acid with initial concentrations (C_0) of 1000 mg/L. The instantaneous adsorbates uptakes on the resin were calculated by measuring the concentrations of adsorbates in solution with UV-Vis spectrometer (UK) at different contact time.

2 Results and discussion

2.1 Characteristics of the polymeric adsorbents

Table 2 lists the characteristics of the adsorbents employed in the current study. Table 2 shows that the hypercrosslinked resin CHA-111 has the largest surface area, micropore area and micropore volume among the four resins but without functional groups on the matrix. The presence of the amino groups on NJ-99 is confirmed by its stronger symmetrical stretching vibration absorbance peaks of C–H of tertiary amino group at 2771 and 2817 cm^{-1}, respectively, and the stretching vibration peaks of C–N at the range 1175–1363 cm^{-1} in the IR spectra in Fig.1b. The presence of the sulfonic group on NG-10 is confirmed by the stronger asymmetrical and symmetrical stretching vibration absorbance peaks of S=O at 1346 and 1265 cm^{-1}, respectively, in Fig.1a. Therefore, it is reasonably considered that the amino group or sulfonic group had been introduced to the surface of the NJ-99 and NG-10, respectively. From Fig.1d, the stronger stretching

Table 2 Physical properties of the four adsorbents

| Property	XAD-4	CHA-111	NJ-99	NG-10
Structure	Polystyrene	Polystyrene hypercrosslinked	Polystyrene, hypercrosslinked with amino groups	Polystyrene, hypercrosslinked with sulfonic groups
Polarity	Non-polar	Weak polar	Moderate polar	Moderate polar
BET surface area (m^2/g)	880.2	934.0	819.1	673.7
Micropore area (m^2/g)	3.1	561.3	463.3	406.5
Micropore volume (ml/g)	0.0051	0.2530	0.209	0.1862
Average pore diameter (nm)	5.83	1.20	1.20	1.26
Quantitative functional groups (mmol/g)	0	0	1.51	1.235
Color	White	Brown	Light brown	Dark brown
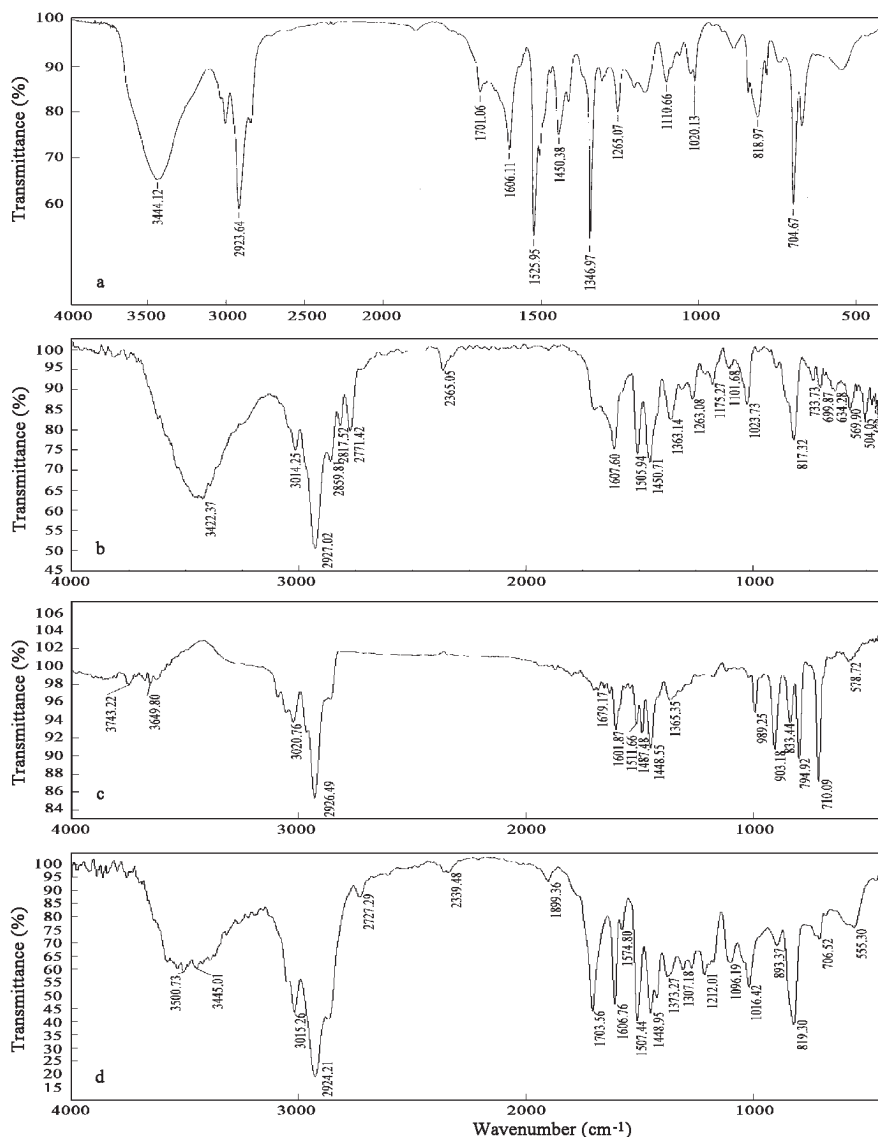
Fig. 1 IR spectra of the polymeric adsorbents. (a) NG-10; (b) NJ-99; (c) XAD-4; (d) CHA-111.

vibration absorbance peak of C═O at 1704 cm^{-1} for CHA-111 demonstrates the presence of C═O in the surface of adsorbent CHA-111, which demonstrates the weak polarity of the adsorbent.

2.2 Equilibrium adsorption

Figure 2 shows the equilibrium adsorption isotherms of *p*-aminobenzoic acid and *o*-aminobenzoic acid on the four adsorbents at 298 K.

The adsorption isotherms at other temperatures (283 K and 313 K) are similar to the isotherms at 298 K. The data are fitted with the empirical Freundlich isotherm equation (Lin and Cheng, 1999):

$$Q_e = K_f C_e^{1/n} \qquad (2)$$

where, K_f and n are the characteristic constants. The correlative isotherm equations along with the relevant parameters are listed in Table 3. The Freundlich isotherm equation can all represent the adsorption data well because all the correlative factors R are larger than 0.99. According to the Freundlich theory (Slejko, 1985), the parameter K_f is taken as a relative indicator of adsorption capacity and $n > 1$ indicates the favorable adsorption. From Table 3, all the exponents (n) in all cases are larger than 1, which demonstrates the adsorption of *p*-aminobenzoic acid and *o*-aminobenzoic acid onto the adsorbents are favorable.

As can be seen from Fig.2 and the fitted Freundlich parameters (Table 3), the order of adsorption capacities of the four polymeric adsorbents for two kinds of aminobenzoic acid is: NJ-99 > CHA-111 > NG-10 > XAD-4.

For an adsorption of aromatic compounds onto polymeric adsorbent from aqueous solutions, the adsorption capacity towards a given adsorbate increases generally

Table 3 Correlated coefficients of the Freundlich adsorption equation (298 K)

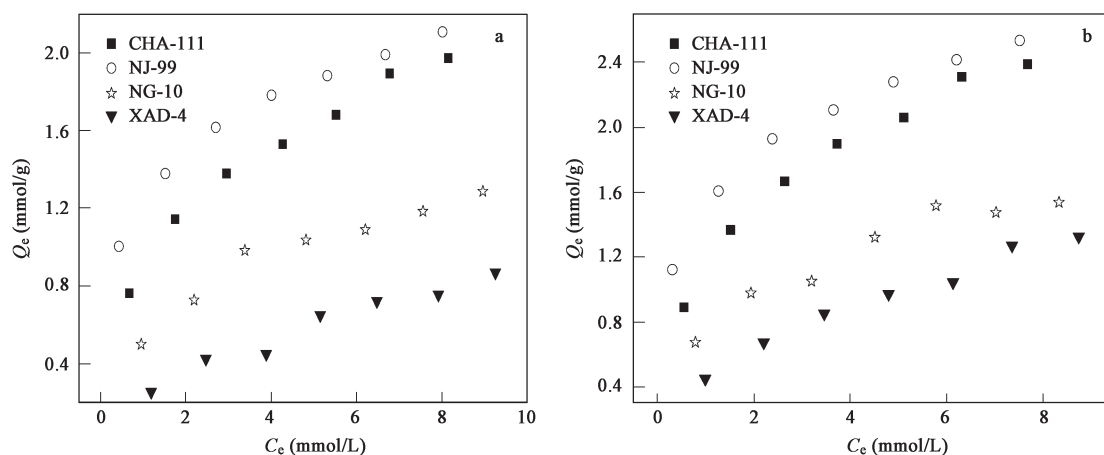| Adsorbent	*p*-Aminobenzoic acid Freundlich parameter			*o*-Aminobenzoic acid Freundlich parameter		
	n	K_f	*R*	*n*	K_f	*R*
CHA-111	2.6309	0.8968	0.9979	2.6497	1.1363	0.9978
NJ-99	3.9370	1.2402	0.9995	3.8941	1.5157	0.9996
NG-10	2.3821	0.5146	0.9981	2.8425	0.7410	0.9915
XAD-4	1.7097	0.2383	0.9956	2.0145	0.4503	0.9963

Fig. 2 Adsorption isotherms of aminobenzoic acid on different adsorbents (298 K). (a) *p*-aminobenzoic acid; (b) *o*-aminobenzoic acid.

as the micropore content and specific surface area of the resin increase (Li *et al*., 2001, 2002). It is evident from Table 2 that the specific surface area of NJ-99 is not the largest, but demonstrates the best adsorption property for aminobenzoic acid. Whereas the adsorbent XAD-4 possesses the bigger surface area and exhibits the smallest adsorption capacity. Hence, the difference may by no means be explained simply by the specific surface area and micropore content. Compared with XAD-4, the hypercrosslinked adsorbents CHA-111, NJ-99 and NG-10 possess the stronger adsorption affinity to aminobenzoic acid, which is primarily attributed to the micropore volume and weak or moderate polarity of the latter three adsorbents. The matching of polarity between adsorbents and adsorbate is an important factor affecting the adsorption of aromatic compounds (Li *et al*., 2001, 2002; Sun *et al*., 2005). For the adsorption of aminobenzoic acid onto NJ-99 and NG-10, the functional groups on the resin may be assumed to play the dominant role. Thus, not only should π–π interactions between the aromatic rings of the adsorbate and the matrix of the resin be taken into account, but also the hydrogen bonding between the functional groups on the resin and the carboxyl or amino groups of aminobenzoic acid (Crittenden *et al*., 1999; Rojas and Voilley, 1996). From Table 2, the amino group content of adsorbent NJ-99 is 1.51 mmol/g. Therefore, the largest adsorption capacity of NJ-99 may be attributed to the amino groups associated with the structure of NJ-99. The amino groups on the resin may undergo the stronger hydrogen bonding with the carboxyl of aminobenzoic acid. Thus, it increases the adsorption capacity of NJ-99 towards the aromatic amphoteric compound containing carboxyl group and simultaneously compensates for the decrease in the adsorption capacity brought out by a decrease in the specific surface area and micropore volume. For NG-10, the stronger hydrogen-bonding interaction occurs between the sulfonic groups of the resin and amino groups of amphoteric adsorbate, but NG-10 presents a smaller adsorption capacity than NJ-99 and CHA-111. This can be explained qualitatively in terms of the functional group content of polymer and specific surface area as well as micropore volume. The functional group content of NG-10

is smaller than NJ-99 (1.235 and 1.51 mmol/g, respectively). All the specific surface area, micropore volume and micropore area of NG-10 are lower than NJ-99 and CHA-111. Therefore, although the formation of hydrogen bonding can increase the adsorption capacity of NG-10, it cannot compensate for the decrease in adsorption capacity owing to the loss of the specific surface area and micropore volume. In a word, specific surface area, micropore structure and content of fuctional groups together dominate the adsorption property of the polymers.

As seen from K_f in Table 3, the adsorption capacities of *o*-aminobenzoic acid on the same adsorbent are all larger than *p*-aminobenzoic acid. The difference in adsorbability can be explained in terms of the adsorbate's solubility, acidity and basicity as well as the position of carboxyl and amino groups on the benzene ring. The solubility of *o*-aminobenzoic acid in water is much lower than *p*-aminobenzoic acid (Table 1) and thus it shows stronger hydrophobicity. This may be one of the possible reasons for its higher adsorption capacity. Further, *o*-aminobenzoic acid possess the lower pK_{a_1} and the higher pK_{a_2} than *p*-aminobenzoic acid (Table 1). Therefore, the Lewis acid-base interaticon between the functional groups of *o*-aminobenzoic acid and the polymers is expected to be stronger than that between *p*-aminobenzoic acid and the resins according to the Lewis acidity and basicity. In addition, some researches (Kumar *et al*., 2003; Sun *et al*., 2005) revealed that the same functional group but at the *ortho* position greatly enhanced the adsorption energies of such compound as *o*-aminobenzoic acid used in the current study. Thus, cumulative effects of solubility and position of the (–COOH) and (–NH$_2$) functional group at the *ortho* position may probably account for higher adsorbalility of *o*-aminobenzoic acid than *p*-aminobenzoic acid onto not only multi-functional polymers but also CHA-111 and XAD-4.

2.3 Adsorption thermodynamics of aminobenzoic acid

To elucidate the adsorption mechanism of aminobenzoic acid onto polymeric adsorbents better, the calculated adsorption thermodynamics parameters according to Eqs. (3)–(5) (Garcla-Delgado *et al*., 1992; John and Tsezos,

Table 4 Calculated thermodynamic parameters at Q_e level of 1.0 mmol/g

Adsorbate	Adsorbent	ΔH (kJ/mol)	ΔG (kJ/mol)			ΔS (J/(mol·K))		
			283 K	298 K	313 K	283 K	298 K	313 K
p-Aminobenzoic acid	CHA-111	−23.14	−6.19	−6.52	−6.53	−59.89	−55.77	−53.07
	NJ-99	−21.45	−8.16	−9.75	−10.48	−46.96	−39.26	−35.05
	NG-10	−18.89	−5.73	−5.90	−5.45	−46.50	−43.59	−42.94
	XAD-4	−19.83	−3.40	−4.23	−3.57	−58.06	−52.35	−51.95
o-Aminobenzoic acid	CHA-111	−21.17	−7.18	−6.56	−6.60	−49.43	−49.03	−46.55
	NJ-99	−13.18	−8.95	−9.65	−9.64	−14.95	−11.85	−11.31
	NG-10	−16.96	−7.42	−7.04	−7.69	−33.71	−33.29	−29.62
	XAD-4	−12.29	−5.14	−4.99	−5.07	−25.27	−24.50	−23.07

1987) are presented in Table 4.

$$\lg(1/C_e) = \lg K_0 + \left(\frac{-\Delta H}{2.303RT}\right) \qquad (3)$$

$$\Delta G = -nRT \qquad (4)$$

$$\Delta S = \frac{\Delta H - \Delta G}{T} \qquad (5)$$

where, C_e is the equilibrium concentration of solution in mmol/L at the absolute temperature T, n is the parameter of the Freundlich equation, ΔH is the isosteric enthalpy change of adsorption, and R is the gas constant, ΔG is the free energy change of adsorption, ΔS is the entropy change of adsorption.

Table 4 shows the adsorption of aminobenzoic acid on the four adsorbents are all the exothermic adsorption process, which is suggested by the negative values of the enthalpy changes. In addition, the absolute values of enthalpy changes are in the 10–30 kJ/mol range indicating the integrated adsorption mechanism involving the π–π interaction, the Van der Waals force and hydrogen-bonding interaction, which suggests the physical adsorption process (Fu *et al.*, 1990; Sun *et al.*, 2005; Zhu *et al.*, 2001). The fact that the adsorption-free energy changes are always negative demonstrates that adsorption of the adsorbate on adsorbents surface is spontaneous. Furthermore, the higher absolute values of free energy changes indicate the higher adsorption property. This difference of free energy changes is consistent with the order of adsorption capacities. The strongest affinity occurs for NJ-99 whereas the weakest affinity occurs for XAD-4 towards the same adsorbate. The negative entropy changes suggest that more ordered arrangement of solute molecules is shaped on the surface of the adsorbent, which are indicative of an enthalpy-driven adsorption process (Pan *et al.*, 2002). The absolute ΔS values decrease with the increase of temperature, which elucidates the rise of temperature augments the randomness at the solid-solution interface during the adsorption process resulting in the increase of entropy after adsorption (Li *et al.*, 2001, 2002; Pan *et al.*, 2002; Sun *et al.*, 2005).

2.4 Adsorption kinetics of aminobenzoic acid

The adsorption kinetics was carried out to explore the practicability in removing aromatic amphoteric compounds from water streams. The effect of contact time (t) on the uptake (Q_t) of *p*-aminobenzoic acid and *o*-aminobenzoic acid onto the four adsorbents in the condition of $C_0 = 1000$ mg/L at 298 K is shown in Fig 3.

The mass transfer effect on the adsorption kinetics can be analyzed by the following Eqs. (6)–(9) (Boyd *et al.*, 1947; Reichenberg, 1953; Hao, 1983).

$$\ln(1 - F) = -R^e t \qquad (6)$$

$$F = \frac{Q_t}{Q_e} = 1 - \frac{6}{\pi^2} \sum_{n=1}^{\infty} \frac{1}{n^2} \exp(-n^2 B_t) \qquad (7)$$

$$\text{when} \quad F > 0.85, \quad Bt = -\ln(1 - F) - 0.4977 \qquad (8)$$

$$\text{when} \quad F < 0.85, \quad Bt = \left(\sqrt{\pi} - \sqrt{\pi - \frac{\pi^2 F}{3}}\right)^2 \qquad (9)$$

where, F is the fractional attainment of equilibrium, R^e and B are the mass transfer coefficients (min⁻¹). The linearity of the plot of $\ln(1-F)$ and t indicates the role of the external mass transfer in the adsorption process. According to Eqs. (8) and (9), the linearity of the plot of
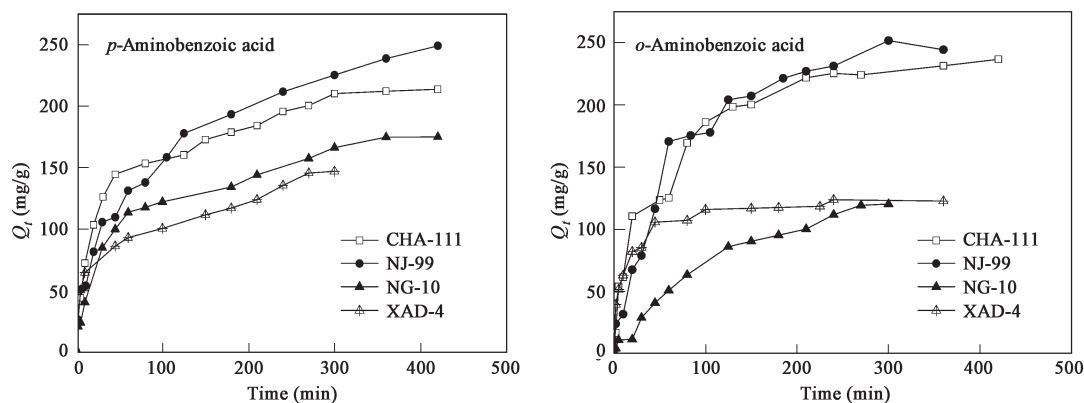

Fig. 3 Adsorption rate curves of aminobenzoic acid onto the four adsorbents at 298 K.

Table 5 Results of the correlated mass transfer equation (298 K)

Adsorbate	Adsorbent	External mass transfer		Intraparticle mass transfer	
		R^e (min^{-1})	R	B (min^{-1})	R
p-Aminobenzoic acid	CHA-111	0.0088	0.9503	0.0070	0.9870
	NJ-99	0.0092	0.9671	0.0057	0.9964
	NG-10	0.0076	0.9587	0.0059	0.9826
	XAD-4	0.0113	0.9366	0.0099	0.9692
o-Aminobenzoic acid	CHA-111	0.0076	0.9012	0.0070	0.9921
	NJ-99	0.0079	0.9543	0.0053	0.9905
	NG-10	0.0083	0.9908	0.0061	0.9645
	XAD-4	0.0176	0.9012	0.0159	0.9736

Table 6 Results of the correlated adsorption kinetic equation

Adsorbent	Temperature (K)	p-Aminobenzoic acid				o-Aminobenzoic acid			
		Pseudo-first order expression		Pseudo-second order expression		Pseudo-first order expression		Pseudo-second order expression	
		K_1[a]	R	K_2[b]	R	K_1[a]	R	K_2[b]	R
CHA-111	283	5.527	0.9650	1.143	0.9990	7.139	0.9850	0.835	0.9961
	298	7.370	0.9841	1.629	0.9962	7.830	0.9726	1.059	0.9969
NJ-99	283	5.527	0.9512	0.709	0.9986	6.679	0.9802	0.686	0.9936
	298	7.370	0.9868	1.013	0.9916	6.909	0.9746	0.766	0.9962
NG-10	283	6.448	0.9856	1.111	0.9871	7.599	0.9874	1.208	0.9776
	298	6.909	0.9752	1.357	0.9948	8.291	0.9910	0.641	0.9824
XAD-4	283	7.600	0.9601	1.864	0.9897	11.28	0.9295	3.155	0.9983
	298	10.36	0.9433	3.176	0.9863	13.82	0.9384	8.205	0.9995

[a] K_1: 10^{-3} min^{-1}, [b] K_2: 10^{-4} g/(mg·min).

Bt against t would show the role of the intraparticle mass transfer. With the kinetic data, the linear fits obtained by plotting $\ln(1-F)$ and t as well as Bt against t are shown in Table 5. The intraparticle diffusion process is a rate-controlling step, because the correlated coefficients R of the intraparticle because mass transfer model are higher than 0.96 (Li *et al.*, 2001, 2002; Pan *et al.*, 2002; Sun *et al.*, 2005). From the correlated results of the intraparticle diffusion process, the diffusion constants (B) of aminobenzoic acid onto macroporous XAD-4 are higher than that onto other hypercrosslinked adsorbents, meaning that the micropore structure is disadvantageous to the adsorption of aminobenzoic acid.

The apparent adsorption rates are examined with the so-called Lagergren equation (Lagergren *et al.*, 1898) and the pseudo-second-order expression (Mckay and Ho, 1999) described as Eqs. (10) and (11).

$$\lg(Q_e - Q_t) = \lg Q_e - \frac{K_1}{2.303}t \qquad (10)$$

$$\frac{t}{Q_t} = \frac{1}{K_2 Q_e^2} + \frac{1}{Q_e}t \qquad (11)$$

where, K_1 is the rate constant of the pseudo-first-order expression (min^{-1}), K_2 is the constant of pseudo-second-order expression (g/(mg·min)). The calculated results are listed in Table 6. From Table 6, the adsorption rate before attaining equilibrium tends to follow the pseudo-second-order kinetics model because of its larger correlation coefficients. The rate constants increase with the temperature indicating that higher temperature could make for a relatively rapid approach to equilibrium. In addition, the apparent adsorption rates (K_2) of the two kinds of aminobenzoic acid onto XAD-4 are both larger than that onto the hypercrosslinked adsorbents, which manifests

the predominating influence of macropore and mesopore on the adsorption rate. This confirms the existence of intraparticle diffusion process as the rate-controlling step.

3 Conclusions

The adsorption capacity of NJ-99 to two kinds of aminobenzoic acid is the largest, and CHA-111 is second, which can be explained by the stronger hydrogen-bonding interaction between the amino groups on the resin and the carboxyl group of aminobenzoic acid as well as micropore volume. The adsorbility of any adsorbent towards o-aminobenzoic acid is larger than p-aminobenzoic acid owing to cumulative effects of the more hydrophobicity of o-aminobenzoic acid as well as the position of carboxyl and amino groups on the benzene ring.

The isotherm data were well fitted with the Freundlich isotherm equation in the conditions of the current study. The thermodynamic results show the exothermic, spontaneous physical adsorption process. Adsorption kinetic studies show that the adsorption conforms to the pseudo-second-order kinetics model and the intraparticle mass transfer process is a rate-controlling step. The quicker attainment of sorption equilibrium (within 4 h) for aminobenzoic acid on NJ-99 is helpful for practical use, and the adsorbent NJ-99 has, therefore, exhibited good potential in removing the aromatic amphoteric compounds from aqueous solutions for industrial purposes.

References

Annadurai G, Krishnan M R V, 1997. Adsorption of acid dye from aqueous solution by chitin: Batch kinetic studies[J]. Indian Journal of Chem Technol, 4: 213–222.

Boyd G E, Adamson A W, Myers L S, 1947. The exchange adsorption of ions from aqueous solutions by organic zeolites. II. Kinetics[J]. J of Am Chem Soc, 69: 2836–2848.

Cai J G, Li A M, Shi H Y *et al.*, 2005. Adsorption characteristics of aniline and 4-methylaniline onto bifunctional polymeric adsorbent modified by sulfonic groups[J]. Journal of Hazard Mater, B124: 173–180.

Crittenden J C, Sanongraj S, Bulloch J L, 1999. Correlation of aqueous-base adsorption isotherm[J]. Environ Sci Technol, 33: 2926–2933.

Fu X C, Shen W X, Yao T Y, 1990. Physical chemistry[M]. Beijing: Higher Education Press.

Garcla-Delgado R A, Cotouelo-Minguez L M, Rodiguez J J, 1992. Equilibrium study of single-solute adsorption of anionic surfactants with polymeric XAD resins[J]. Sep Sci Technol, 27: 975–987.

Hao B C, 1983. The base and design of adsorption[M]. Beijing: Chemistry Industrial Press.

He B L, Huang W Q, 1995. Ion exchange and adsorption resins[M]. Shanghai: Shanghai Science and Technology Press.

Ho Y S, Mckay G, 1999. Comparative sorption kinetic studies of dye and aromatic compounds onto fly ash[J]. J Environ Sci Health, A34: 1179–1204.

John P B, Tsezos M, 1987. Removal of hazardous organic pollutants by biomass adsorption[J]. Journal of Water Pollut Control Fed, 59: 191–198.

Kumar A, Kumar Shashi, Kumar Surendra, 2003. Adsorption of resorcinol and catechol on granular activated carbon: Equilibrium and kinetics[J]. Carbon, 41: 3015–3025.

Lagergren S, 1898. Zur theorie der sogenannten adsorption geloster stoffe[M]. Handlingar: Kungliga Svenska Vetenskapsaka-demiens.

Li P, Arup K SenGupta, 2000. Intraparticle diffusion during selective ion exchange with a macroporous exchanger[J]. Reactive and Functional Polymers, 44: 273–287.

Li A M, Zhang Q X, Chen J L *et al.*, 2001. Adsorption of phenolic compounds on Amberlite XAD-4 and its acetylated derivative MX-4[J]. React Funct Polym, 49: 225–233.

Li A M, Zhang Q X, Zhang G C *et al.*, 2002. Adsorption of phenolic compounds from aqueous solutions by a water-compatible hypercrosslinked polymeric adsorbent[J]. Chemosphere, 47: 981–989.

Lin S H, Cheng Y H, 1999. Adsorption of BTEX from aqueous solution by macroreticular resins[J]. Journal of Hazard Mater, 70: 21–37.

Lin C K, Tsai T Y, Liu J C *et al.*, 2001. Enhanced biodegradation of petrochemical wastewater using ozonation and bac advanced treatment system[J]. Wat Res, 3: 699–704.

Liu G Q, Ma L X, Liu J, 2002. Handbook of chemistry and chemical engineering physical data[M]. Beijing: Chemical Engineering Press.

Mckay G, Ho Y S, 1999. Pseudo-second order model for sorption process[J]. Process Biochem, 34:451–465.

Pan B C, Xiong Y, Li A M *et al.*, 2002. Adsorption of aromatic acids on an aminated hypercrosslinked macroporous polymer[J]. React Funct Polym, 53: 63–72.

Pan B C, Zhang X, Zhang W M *et al.*, 2005. Adsorption of phenolic compounds from aqueous solution onto a macroporous polymer and its aminated derivative: isotherm analysis[J]. Journal of Hazard Mater, B121: 233–241.

Reichenberg D, 1953. Properties of Ion-exchange resins in relation to their structure III, Kinetics of exchange[J]. J Am Chem Soc, 75: 589–597.

Rojas J A, Voilley A, 1996. Trapping of aromatic compounds by adsorption on hydrophobic sorbents[J]. Sep Sci Technol, 31: 2473–2491.

Slejko F L, 1985. Adsorption Technology: A step-by-step approach to process evaluation and application[M]. New York: Marcel Dekker.

Sun Y, Chen J L, Li A M *et al.*, 2005. Adsorption of resorcinol and catechol from aqueous solution by aminated hypercrosslinked polymers[J]. Reactive & Functional Polymers, 64: 63–73.

Zhang P F, Wang Y P, Li W *et al.*, 1999. Treatment of waster from Intermediate *p*-aminophenol manufacturing process with ferrous-hydrogen peroxide method[J]. Chemical Industry and Engineering, 6: 330–334.

Zhang Q L, Chuang K T, 2001. Adsorption of organic pollutants from effluents of a Draft pulp mill on activated carbon and polymer resins[J]. Advance in Environ Res, 3 : 251–258.

Zhu L Z, Yang K, Xu G J, 2001. Characters of *p*-nitrophenol sorption in sediments-sorption isotherms and sorption thermodynamics[J]. Acta Scientiae Circumstantiae, 21: 674–678.